

A Band of Critical States in Anderson Localization at Strong Magnetic Field with Random Spin-Orbit Scattering

C. Wang^{1,2}, Ying Su^{1,2}, Y. Avishai^{3,*}, Yigal Meir³, and X. R. Wang^{1,2†}

¹Physics Department, The Hong Kong University of Science and Technology, Clear Water Bay, Kowloon, Hong Kong

²HKUST Shenzhen Research Institute, Shenzhen 518057, China and

³Department of Physics, Ben-Gurion University of the Negev Beer-Sheva, Israel

(Dated: June 24, 2021)

Anderson localization problem for non-interacting two-dimensional electron gas subject to strong magnetic field, disordered potential and spin-orbit coupling is studied numerically on a square lattice. The nature of the corresponding localization-delocalization transition and the properties of the pertinent extended states depend on the nature of the spin-orbit coupling (uniform or fully random). For uniform spin-orbit coupling (such as Rashba coupling), there is a band of extended states in the center of a Landau band as in a “standard” Anderson metal-insulator transition. However, for *fully random* spin-orbit coupling, the familiar pattern of Landau bands disappears. Instead, there is a *central band of critical states with definite fractal structure* separated at two critical energies from two side bands of localized states. Moreover, finite size scaling analysis suggests that for this novel transition, on the localized side of a critical energy E_c , the localization length diverges as $\xi(E) \propto \exp(\alpha/\sqrt{|E - E_c|})$, a behavior which, along with the band of critical states, is reminiscent of a Berezinskii-Kosterlitz-Thouless transition.

PACS numbers: 71.30.+h, 73.20.Jc

Traditionally, non-interacting disordered electronic systems subject to disordered potential are classified according to the symmetries of their Hamiltonian with respect to time reversal (TR) and spin rotation (SR) transformations. Considering the Hamiltonian as a random matrix [1–3], its symmetries determine to which random matrix Gaussian ensemble (also referred to as universality class) it belongs, orthogonal (both TR and SR symmetries are satisfied), symplectic (only TR symmetry) or unitary.

This classification is intimately related to one of the most fundamental concepts in the physics of disordered electronic systems: the Anderson localization transition (ALT) [4, 5] that is a *quantum phase transition* between localized and extended states in a disordered system. The critical dimension for existence or non-existence of ALT is $d = 2$. For $d < 2$ there is no ALT while for $d > 2$ there is always ALT. Hence, for two-dimensional electron gas (2DEG), ALT (if it exists) is of special interest. The scaling theory of localization [6] (developed before the discovery of the quantum Hall effect) together with calculations based on nonlinear sigma model [7, 8], established that for $d = 2$, ALT does not exist for the orthogonal and unitary classes (zero or finite magnetic field, respectively) and does exist for the symplectic class (finite spin-orbit scattering and zero magnetic field). After the discovery of the integer Quantum Hall effect (IQHE) [9], topology was also recognized as a property determining the pertinent universality class [10]. Mathematically, the role of topology in the IQHE is quantified by the occurrence of a topological term in the action of the corresponding non-linear sigma model[11]. In the presence of the topological term it is established that *if SR invariance is respected*, the system is in the IQHE universality class

characterized by a Hall transition between localized and critical states occurring at discrete energies. What is less clear (and motivates the present study) is what happens in the presence of the topological term *when SR invariance is broken*. To the best of our knowledge, there is so far no rigorous extension of the non-linear sigma model for an IQHE system in the presence of strong spin-orbit coupling (SOC).

In this work we investigate (numerically) the nature of transition between localized and extended states for a disordered 2DEG subject to strong (perpendicular) magnetic field in which SR invariance is broken due to SOC. In Ref. [12], the nature of states between Zeeman split states of the first and second Landau levels was investigated for weak random SOC, and a percolation like ALT transition has been established. Here we neglect the Zeeman energy and show that the nature of the SOC (uniform or fully random) dramatically affects the pertinent transition. Our main results are: 1) For *uniform* SOC (such as Rashba coupling due to a uniform electric field), the pattern of separated Landau bands persists. Focusing attention on the lowest Landau band centered at an energy E_0 , it is shown that there are two energies $E_{c_1} < E_0 < E_{c_2}$ that are critical in the sense that the states $\psi_E(\mathbf{r})$ for $E_{c_1} < E < E_{c_2}$ are *metallic*, while for $E \notin [E_{c_1}, E_{c_2}]$, they are localized. This is a “usual” ALT between a band of localized states and a band of metallic states. Finite size scaling analysis indicates that the critical exponent for the divergence of the localization length is close to that of the IQHE. 2) However, for *fully random* spin-orbit coupling, the structure of broadened Landau bands that is the hallmark of the IQHE is completely washed out. In turn, there is a broad *band of critical states* with definite fractal structure (the frac-

tal dimension equals 1.82 ± 0.02). This band is separated in two critical energies $E_{c_1} < E_{c_2}$ from two narrow side bands of localized states. Finite size scaling analysis suggests that for this novel transition, the localization length at energy E (on the localized side) diverges as $\xi(E) \propto \exp(\alpha/\sqrt{|E - E_c|})$, a behavior reminiscent of a Berezinskii-Kosterlitz-Thouless (BKT) transition [13].

To substantiate our claims we consider a tight-binding Hamiltonian for 2DEG on a square lattice of length L and width M (the lattice constant is set to unity),

$$H = \sum_{i,\sigma} \epsilon_i c_{i,\sigma}^\dagger c_{i,\sigma} + \sum_{\langle ij \rangle, \sigma, \sigma'} \exp(i\phi_{ij}) V_{ij}(\sigma, \sigma') c_{i,\sigma}^\dagger c_{j,\sigma}. \quad (1)$$

Here $i = (n_i, m_i)$ is a lattice site specified by integer coordinates n_i and m_i with $1 \leq n_i \leq L$ and $1 \leq m_i \leq M$. $c_{i,\sigma}^\dagger$ ($c_{i,\sigma}$) is electron creation (annihilation) operator of spin $\sigma = \pm$ on site i . The on-site energy ϵ_i are random and uniformly distributed in the range of $[-W/2, W/2]$, so that W measures the degree of randomness. The symbol $\langle ij \rangle$ indicates that i and j are nearest neighbor sites. The magnetic field is introduced through the Peierls' substitution [14] by endowing the hopping coefficient with a phase, $\phi_{ij} = \frac{e}{\hbar} \int_i^j \vec{A} \cdot d\vec{l}$, where \vec{A} is the vector potential. For a constant magnetic field B the sum of phases along four links around a square (the same for all squares) is written as $2\pi\phi$, where ϕ is the magnetic flux per square in units of the quantum flux $\Phi_0 = ch/e$. Henceforth, the magnetic field B is expressed in terms of ϕ .

The SOC is encoded by 2×2 matrices V_{ij} acting in spin space. We will explore both the case of constant SOC matrices along the axes and the case of fully random SOC matrices. In the case of constant SOC matrices, they are parametrized as $V_{ij} = V_x$ (V_y) for $\langle ij \rangle$ along the x -direction (y -direction). In order to get non-trivial results due to SOC, one requires $[V_x, V_y] \neq 0$.

The Rashba form of uniform SOC reads,

$$V_x = \begin{bmatrix} 1 & a \\ -a & 1 \end{bmatrix} \quad \text{and} \quad V_y = \begin{bmatrix} 1 & -ia \\ -ia & 1 \end{bmatrix}, \quad (2)$$

where a is a real constant encoding the strength of the SOC for the Rashba model. Random SOC is encoded by matrices $V_{ij} \in \text{SU}(2)$ thereby defining the $\text{SU}(2)$ model [15],

$$V_{ij} = \begin{bmatrix} e^{-i\alpha_{ij}} \cos(\beta_{ij}/2) & e^{-i\gamma_{ij}} \sin(\beta_{ij}/2) \\ -e^{i\gamma_{ij}} \sin(\beta_{ij}/2) & e^{i\alpha_{ij}} \cos(\beta_{ij}/2) \end{bmatrix}, \quad (3)$$

where α_{ij} , β_{ij} and γ_{ij} are random angles. In the full $\text{SU}(2)$ model studied here, α_{ij} and γ_{ij} are uniformly distributed in $[0, 2\pi]$ and $\sin(\beta_{ij})$ is uniformly distributed in $[0, 1]$.

Localization-delocalization transition in an electronic system at zero temperature is characterized not only by

divergence of the localization length but also by the nature of the wave functions $\psi_{E_c}(\mathbf{r})$ at the critical energies. These two criteria are independent of each other, and their analysis usually require two different numerical procedures.

Study of the localization properties: We consider a scattering problem for an electron at Fermi energy E living on a square lattice of length $L \rightarrow \infty$ (along x) and finite width M (along y). Periodic boundary conditions are imposed along y to avoid edge states contribution.

Since the system is quasi one-dimensional, it has a finite localization length $\lambda_M(E)$ depending on the energy and the system's width M . Using the transfer matrix method we calculate $\lambda_M(E)$ by a standard iteration algorithm [4, 16]. In our calculations $L > 10^6 \gg \lambda_M(E)$ and self-averaging requires relatively small data ensembles to achieve good statistics. The width M takes values between 32 and 96. Denoting the normalized localization length by $\bar{\lambda}_M(E) \equiv \lambda_M(E)/M$, the identification of a transition point E_c on the energy axis is guided by the following observations: 1) For metallic (insulating) scattering states, $\bar{\lambda}_M(E)$ is an increasing (decreasing) function of M . 2) For critical states, $\bar{\lambda}_M(E)$ is independent of M . 3) For energy E close to a critical point E_c , $\bar{\lambda}_M(E)$ obeys a single parameter finite size scaling. Explicitly, let us denote by $\xi(E) \equiv \lambda_\infty(E)$ the localization length for a system of width $M \rightarrow \infty$. At the critical energy we expect $\xi(E_c) = \infty$, and finite size scaling implies $\lambda_M(E) = f[\frac{M}{\xi(E)}]$ where $f(x)$ is a universal (disorder independent) scaling function.

The constant SOC case, Eq. (2): In this case, the pattern of separate LBs remains intact, and our attention is focused on the lowest LB. The upper panel of Fig. 1(a) displays the quantity $\ln \bar{\lambda}_M(E)$ v.s E for $B = 1/5$ and $W = 1$ in the *absence* of the SOC, that is, $a = 0$. It is evident that all curves for different widths M coalesce at the peak energy E_c . On both sides of E_c , $\ln \bar{\lambda}_M(E)$ *decreases* with M , indicating that all states away from E_c are localized. However, at the critical point E_c , $\bar{\lambda}_M(E)$ is independent of M , and the corresponding states are critical [17]. The bottom panel displays $\ln \bar{\lambda}_M(E)$ for the same values of B and W as in the upper panel when the constant (Rashba) SOC strength is $a = 0.1$. Here, in contradistinction from the case of zero SOC, curves of different M cross at *two energies* ($E_{c,1} = -2.91 \pm 0.01$, $E_{c,2} = -2.99 \pm 0.01$). Moreover, states between these two points are *metallic* because $\ln \bar{\lambda}_M(E)$ *increases* with M , indicating that these are metallic extended states (the corresponding wavefunctions have a trivial fractal structure as for plane-waves).

Now we use the hypothesis of single parameter finite size scaling to substantiate the criticality of the transition, namely, that for E close to $E_{c,i}$ $\bar{\lambda}_M(E) = f[\frac{M}{\xi(E)}]$. The results are summarized in Fig. 1(b,c). As shown in

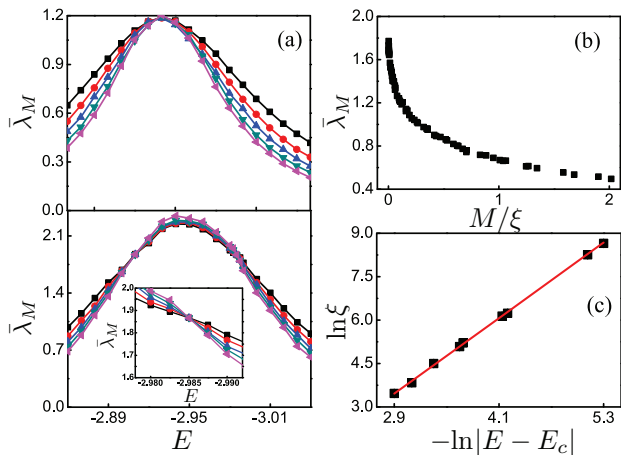


FIG. 1: (Color online) $\bar{\lambda}_M(E)$ (averaged over 40 disorder realizations), *v.s.* E for $B = 1/5$ and $W = 1$. (a) Without SOC (upper panel) and with constant Rashba SOC, Eq. (2) with $a = 0.1$, (bottom panel). The system widths (from top to bottom) are $M = 32$ (square), 48 (circle), 64 (up-triangle), 80 (down-triangle), and 96 (left-triangle). The inset of the bottom panel is a zoom in on the crossing region around $E_c = -2.985$. (b) When the points $\bar{\lambda}_M(E)$ shown in (a) are expressed in terms of $x = M/\xi(E)$ (where the localization length $\xi(E)$ is derived through the numerical procedure), they fall on a smooth curve thereby display the scaling function. (c) $\ln \xi(E)$ *v.s.* $\ln |E - E_c|$, $E_c = -2.985$, for the constant Rashba SOC. The solid line is linear fit with slope (critical exponent) $\nu = 2.2$.

Fig. 1(b), in the vicinity of the crossing points, all data points $\bar{\lambda}_M(E)$ for the Rashba SOC case collapse onto a single smooth scaling curve $f(x)$. Like in the standard ALT or Hall transitions, $\xi(E)$ diverges as a power, $|E - E_c|^{-\nu}$, with ν the localization length critical exponent. This is substantiated in Fig. 1(c) that displays $\ln \xi(E)$ *v.s.* $\ln |E - E_c|$ for the Rashba SOC case, Eq. (2). The fit to a straight line is rather satisfactory, yielding a slope $\nu_1 = 2.2 \pm 0.1$, that is somewhat smaller than both critical exponents of the 2D disordered systems $\nu \simeq 2.75$ for the 2D symplectic symmetry class [15] and $\nu \simeq 2.34$ for the IQHE [5].

Localization for the fully random SU(2) model, Eq. (3):
 In the absence of a magnetic field, the SU(2) model supports a standard ALT as shown in the upper panel of Fig. 2(a) which plots $\ln(\bar{\lambda}_M(E))$ *v.s.* E for $W = 1$ and various M . All curves cross at $E_c = -3.259$, showing all states of $E \in [-3.259, 3.259]$ are extended because $\ln(\bar{\lambda}_M(E))$ increases with M as shown clearly in the inset of the enlarged crossing region. Finite size scaling yields the value $\nu = 2.73 \pm 0.02$ commensurate with earlier calculations [15].

We come now to the main result of the present work. Switching a strong magnetic field $B = 1/5$ one would expect a pattern of LB modified due to the presence of SOC. However, what we find is that the curves $\bar{\lambda}_M(E)$ do not display separate LB peaks, but, rather, a single

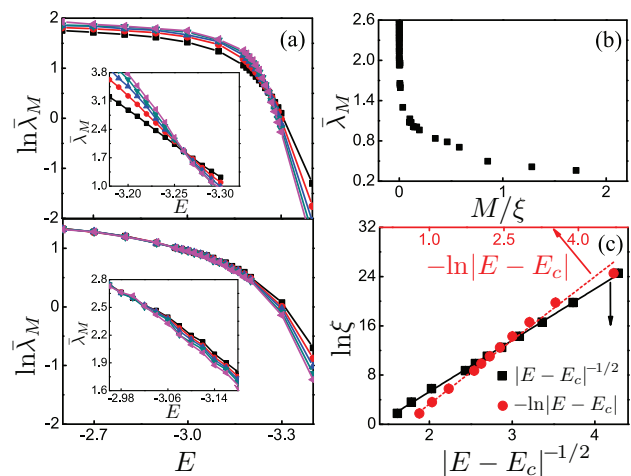


FIG. 2: (color online) (a) $\ln(\bar{\lambda}_M)$ *v.s.* E of the SU(2) model with $W = 1$ and $M = 32$ (square); 48 (circle); 64 (up-triangle); 80 (down-triangle); 96 (left-triangle). The top panel is for $B = 0$, and the inset is a zoom in on the crossing region in linear scale. The bottom panel is for $B = 1/5$, and the inset is a zoom in on the merging region. (b) The scaling function obtained from the bottom panel in (a) by collapsing data of $\bar{\lambda}_M$ near the merging point into a single curve. (c) $\ln \xi$ *v.s.* $|E - E_c|^{-1/2}$ for $E_c = -3.001$ (squares). The solid line is a linear fit with slope $\alpha = 8.3 \pm 0.3$. For a comparison, $\ln \xi$ *v.s.* $-\ln |E - E_c|$ with $E_c = -3.051$ (circles) is also plotted. Larger deviation in the linear fit (dashed line with goodness-of-fit of 5.2×10^{-7}) indicates that an interpretation in terms of BKT-type transition (with goodness-of-fit of $8. \times 10^{-3}$) explains the data better.

band. More remarkably, in contradistinction with the symplectic case (SOC and $B = 0$), the curves $\bar{\lambda}_M(E)$ that display a localized region for energies $\{E\}$ near the band edge (that is, $\bar{\lambda}_M(E)$ decreases with M), *do not cross but merge* as the energy approaches the band center. This is evident by looking at the bottom panel of Fig. 2(a) that displays $\ln(\bar{\lambda}_M(E))$, averaged over 40 ensembles, as a function of E for $B = 1/5$, $W = 1$ and various system widths M . The inset is a zoom in of the merging region. For $E < E_c = -3.001$ the system behaves as an insulator where $\bar{\lambda}_M(E)$ decreases with M . But for $E \geq E_c$ all curves merge, forming a band of critical states for which $\bar{\lambda}_M(E)$ is independent of M , and, as we shall see below, the corresponding wave-functions cover only a fractal part of 2D space. This band of critical states prevails for all energies $|E| < |E_c| = 3.001$, namely the pattern of separate Landau bands is completely washed out.

To explore the nature of this localization-delocalization transition we inspect the behavior of $\xi(E)$ on the insulating side $E < E_c$. Fig. 2(b) depicts the collapse of all curves $\bar{\lambda}_M(E)$ for different widths M , supporting the quantum phase transition interpretation. However, if one analyzes the divergence of ξ in terms of a power law, as shown by the red dotted line in the log-log plot in Fig. 2(c), the goodness-of-fit [18] to the numerical data

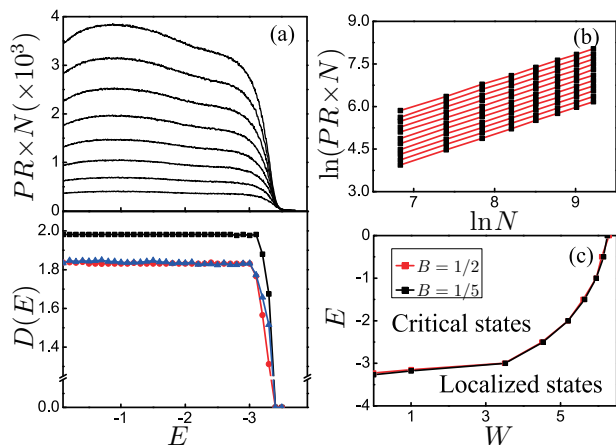


FIG. 3: (color online) (a) Upper panel: $PR(E) \times N$, averaged over 100 samples, as a function of E of the SU(2) model, Eq. (3), for $B = 1/5$ and $W = 1$. The lattice size (from down up) is $M = 30; 40; 50; 60; 70; 80; 90; 100$. Lower panel: $D(E)$ *v.s* E for $W = 1$ and $B = 0$ (black square); $B = 1/5$ (red circle); $B = 1/2$ (blue triangle). (b) The quantity $\ln(PR(E) \times N)$ is plotted *v.s* $\ln N$ for $E = -2.9, -2.8, \dots, -2$. The solid lines are the linear fits of the data with slopes 0.91 ± 0.01 . (c) Phase diagram of the SU(2) model for $B = 1/2$ (red circle) and $B = 1/5$ (black square) in the $E - W$ plane. Above $W_c = 6.3$, all states are localized.

(red circles) is about 5.2×10^{-7} , which is four orders of magnitude smaller than an acceptable value. Moreover, the resulting exponent turns out to be $\nu \simeq 6.4$, much larger than any known critical exponent in these kind of systems. The occurrence of a line of critical points in our 2D system is reminiscent of a critical behavior of the BKT phase transition [13], $\xi(E) \propto \exp(\alpha/\sqrt{|E_c - E|})$. Indeed, the fit to a straight line in Fig. 2(c), which displays $\ln \xi$ against $1/\sqrt{|E - E_c|}$, supports the assertion of BKT-type transition [16]. Quantitatively, the corresponding goodness-of-fit to the numerical data (black squares) is about $8. \times 10^{-3}$, far better than the power-law fit, thereby supporting our claim.

Fractal structure of critical states: To confirm the criticality of all states along the merging line, we compute, by exact diagonalization, the normalized electron wave functions $\psi_E(i)$ on a square lattice of *finite extent* (for convenience we take a rectangle of area $M(M+1)$). Here $i = (n_i, m_i) = 1, 2, \dots, N = M(M+1)$ is a site on this lattice). According to our previous discussion, the wave functions for energies $E > -3.001$ belong to the band of critical states. Their fractal nature can be confirmed by computing the participation ratio,

$$PR(E) = \frac{1}{N \sum_i |\psi_E(i)|^4}. \quad (4)$$

For a state whose wave-function occupies a fractal space of dimension $D(E)$ [19], PR scales with N as $PR \propto N^{-1+D(E)/2}$, with $D(E) \geq 0$. For a localized state,

$PR \propto N^{-1}$. The upper panel of Fig. 3(a) displays $PR \times N$ as a function of energy for $B = 1/5$, $W = 1$ (same as those in Fig. 2) and various M . All curves merge for $E < E_c$ (localized region), showing the independence of energy of $PR \times N$. Thus those wavefunctions of energy less than E_c are indeed localized. For $0 \geq E > E_c$, $PR \times N$ increases with M . To demonstrate that these states are critical with a non-trivial fractal structure, Fig. 3(b) displays $\ln[PR]$ against $\ln N$ for 10 different energies $E = -2.9; -2.8; -2.7; \dots; -2$. They are almost parallel to each other with a common slope of 0.91 ± 0.01 , indicating fractal wave-functions of fractal dimension $D(E) = 1.82 \pm 0.02$ for those states.

The fractal nature of the critical states is universal in the sense that $D(E)$ does not depend neither on the magnetic field (as long as it is strong enough) nor on energy (as long as $E > E_c$). This is substantiated in the bottom panel of Fig. 3 (a) where $D(E)$ is plotted *v.s* E for $W = 1$ and $B = 1/5$ (red circles) and $B = 1/2$ (blue triangles). It is instructive to compare the fractal properties of the critical wave-functions discussed above with those of the wave-functions for the SU(2) model *at zero magnetic field* (that is, the metallic side for the symplectic ensemble). The fractal dimension of these wave-function as a function of E is also shown in the bottom panel of Fig. 3(a) (black squares). In contrast with the case $B = 1/5$ for which the fractal dimension is shown to be 1.82 ± 0.02 , the extended states in the absence of the field are metallic ($D(E) = 2$) and occupy the entire lattice. Our fractal dimension is somewhat bigger than $D = 1.75$ for the critical state of IQHE systems [20] and $D = 1.66 \pm 0.05$ for the critical state of SU(2) model at zero field [21].

The critical point E_c that marks the edge of the band of critical states clearly depends on the strength of disorder W . The larger is W , the smaller is E_c . On the other hand, for strong enough field, E_c is virtually independent on the magnetic field. It is then useful to draw a phase diagram of the SU(2) model where the line $E_c(W)$ separates regions of localized and critical states. This analysis is carried out and the result is presented in Fig. 3(c) where $E_c(W)$ is plotted *v.s* W for $B = 1/5$ (black squares) and $B = 1/2$ (red circles). The fact that for $W \geq 6.5$ all states are localized (albeit in the absence of SOC), has already been substantiated[17].

In conclusion, the nature of ALT for 2DEGs with potential disorder and SOC subject to a strong perpendicular magnetic field depends on whether the SOCs is realized by constant or fully random SU(2) matrices operating in spin space. For constant SOC, (such as in the Rashba term induced by a uniform electric field, Eq. (2)), there is a normal ALT separating localized and extended states that form a band of finite width. The corresponding critical exponent is similar to that obtained in the absence of magnetic field for the symplectic ensemble. On the other hand, for the fully random SU(2) model of the SOC, Eq. (3), the pattern of separated LBs is

smearred and the system undergoes a BKT-type transition separating localized states from critical states. The localization length diverges as an exponential of an inverse square root and the critical states form a band of finite width and occupy a fractal space whose dimension is about 1.82. This is in contrast with zero field case, where in the presence of fully random spin-orbit scattering the system undergoes a regular ALT separating localized states from extended (metallic) states.

This work is supported by NSFC of China grant (11374249) and Hong Kong RGC grants (605413). YA would like to thank the Physics Department of HKUST for hospitality during 2012-2014. The research of YA is partially supported by Israeli Science Foundation Grants 1173/2008 and 400/2012.

* corresponding author: yshai@bgumail.bgu.ac.il

† corresponding author: phxwan@ust.hk

- [1] E. P. Wigner, *Group Theory and its Application to the Quantum Mechanics of Atomic Spectra*, Academic Press, New York, 1959.
- [2] F. J. Dyson, *J. Math. Phys.* **3**, 140 (1962); **3**, 157 (1962); **3**, 166 (1962).
- [3] M. L. Mehta, *Theory of Random Matrices*.
- [4] B. Kramer and A. Mackinnon, *Rep. Prog. Phys.* **56**, 1469(1993).
- [5] B. Huckestein, *Rev. Mod. Phys.* **67**, 357 (1995).
- [6] E. Abrahams, P. W. Anderson, D. C. Licciardello and T. V. Ramakrishnan, *Phys. Rev. Lett.* **42**, 673(1979).
- [7] D. Friedan, *Phys. Rev. Lett.* **45**, 1057 (1980).
- [8] S. Hikami, A.I. Larkin and Y. Nagaoka, *Prog. Theor. Phys.* **63**, 707 (1980).
- [9] *The Quantum Hall Effect*, edited by R. E. Prange and S. M. Girvin (Springer-Verlag, New York, 1990).
- [10] D. J. Thouless, M. Kohmoto, M. P. Nightingale, and M. den Nijs, *Phys. Rev. Lett.* **49**, 405 (1982).
- [11] H. Levine, S. B. Libby and A. M. M. Pruisken, *Nuclear Physics B* **240**, 30 (1984).
- [12] Y. Avishai and Y. Meir, *Phys. Rev. Lett.* **89**, 076602 (2002).
- [13] V. L. Berezinskii, *Sov. Phys. JETP* **32**, 493(1971); J. M. Kosterlitz and D. J. Thouless, *J. of Phys. C* **6**, 1181(1973).
- [14] X. R. Wang, *Phys. Rev. B* **51**, 9310(1995); *ibid.* **53**, 12035(1996).
- [15] Yoichi Asada, Keith Slevin and Tomi Ohtsuki, *Phys. Rev. Lett.* **89**, 256601 (2002).
- [16] X. C. Xie, X. R. Wang and D. Z. Liu, *Phys. Rev. Lett.* **80**, 3563(1998).
- [17] C. Wang, Y. Avishai, Y. Meir, and X.R. Wang, *Phys. Rev. B* **89**, 045314(2014).
- [18] *Numerical Recipes in Fortran 77*, 2nd Edition, W. H. Press, S. A. Teukolsky, W. T. Vetterling, and B. P. Flannery (Cambridge University Press, 1996).
- [19] X. R. Wang, Y. Shapir, and M. Rubinstein, *Phys. Rev. A* **39**, 5974(1989).
- [20] F. Evers, A. Mildenberger, and A. D. Mirlin, *Phys. Rev. B* **67**, 041303 (2003).
- [21] H. Obuse, K. Yakubo, *Phys. Rev. B* **69**, 125301 (2004).